BNL-29048

Numerical Techniques for Lattice Gauge Theories

by

Michael Creutz*

Abstract

I review the motivation for formulating gauge theories on a lattice. Then I discuss Monte Carlo simulation techniques for these systems. Finally, the Monte Carlo methods are combined with renormalization group analysis to give strong numerical evidence for confinement of quarks by non-Abelian gauge fields.

February 6, 1981

*Lectures for the XVIIIth Karpacz Winter School of Theoretical Physics, Karpacz, Poland, February 19-March 4, 1981.

DISCLAIMER

Numerical Techniques for Lattice Gauge Theories

by

Michael Creutz*

Abstract

I review the motivation for formulating gauge theories on a lattice. Then I discuss Monte Carlo simulation techniques for these systems. Finally, the Monte Carlo methods are combined with renormalization group analysis to give strong numerical evidence for confinement of quarks by non-Abelian gauge fields.

February 6, 1981

*Lectures for the XVIIIth Karpacz Winter School of Theoretical Physics, Karpacz, Poland, February 19-March 4, 1981.

Abstract

I review the motivation for formulating gauge theories on a lattice. Then I discuss Monte Carlo simulation techniques for these systems. Finally, the Monte Carlo methods are combined with renormalization group analysis to give strong numerical evidence for confinement of quarks by non-Abelian gauge fields.

I. Introduction

Fusing quantum mechanics and special relativity, quantum field theory persists as the dominant tool in elementary particle theory. However, the nulcear force remains enigmatic in the lack of an obvious small parameter permitting perturbative calculation. Despite the paucity of precise predictions, the conviction is growing that the strong interactions arise in a local Yang-Mills theory of non-Abelian gauge fields interacting with quarks.[1] In this conventional picture the strong interaction theory differs in one striking aspect from all other physical applications of gauge fields. Only here is it necessary that the spectrum of states not include free particles with the quantum numbers of the elementary fields used to define the theory. The non-observation of free quarks and massless gauge gluons leads us to ask that their physical manifestation be through the hadrons which are gauge singlet bound states.

Current theoretical evidence that a non-Abelian gauge theory can display this phenomenon of "confinement" is remarkably sparse. Perturbation theory, historically the primary tool of the field theorist, has thus far failed to give any clear signals of quark imprisonment. Renormalization group arguments suggest that at large quark separation, where confinement becomes important, the effective coupling constant of the theory becomes large and perturbative techniques may break down. Recent studies of classical solutions to non-Abelian gauge theory suggest important non-perturbative quantum effects at large distances.[2]

A computational complication of quantum field theory is the presence of ultraviolet divergences. From a perturbative point of view, we have a multitude of regularization schemes for controlling these infinities. Physical quantities, such as the anamalous magnetic moment of the electron, should possess a finite limit independent of renormalization scheme as cutoff is removed.

To study a non-perturbative phenomenon such as confinement, we require a non-perturbative regulator. This precludes most of the conventional schemes which are based on the Feynman expansion. Herein

lies the virtue of a lattice formulation. As wavelengths less than twice the lattice spacing a have no meaning, a lattice represents a cutoff of each momentum component at π/a. This cutoff is totally free from any perturbative expansion.

As with any cutoff, considerable ambiguity remains in a lattice formulation. Upon removal of the cutoff, the physics of a renormalizable field theory should be independent of the details of the regulator. However, when the lattice is in place, one is free to add to the Lagrangian terms which will not contribute in the continuous limit. Using this freedom, Wilson has presented a particularly elegant lattice formulation of gauge theories. His prescription keeps exact local gauge symmetry in a mathematically well defined system. Furthermore, in the strong coupling limit his formalism yields confinement; there the theory describes quarks connected by strings carrying a finite energy per unit length.

Ultimately interest lies in the continuous limit of the theory. In this limit physical scales, for example the Compton wavelengths of the hadrons, go to infinity relative to the lattice spacing. In the language of statistical mechanics, this represents the expected behavior at a critical point, where correlation lengths in lattice units diverge. For the non-Abelian gauge theory of the strong interaction, renormalization group analysis indicates such a critical point at vanishing bare coupling constant. A continuum limit utilizing this point yields the phenomenon of asymptotic freedom; the effective renormalized coupling becomes small logarithmically with the scale on which it is defined. The interest in this phenomenon is the prediction of the

scaling behavior apparently observed in high momentum transfer processes such as deeply inelastic electron-proton scattering.

Thus arises the desire for non-Abelian gauge theories simultaneously to confine quarks and to exhibit asymptotic freedom. This simple picture would be precluded if the corresponding lattice theory possesses a further critical point at a phase transition separating the small coupling regime of asumptotic freedom from the strong coupling regime where Wilson's expansion indicates confinement.[4] It is the theorists task to show that SU(3) lattice gauge theory in four space-time dimensions exhibits no phase transition except at zero coupling.

Disconcertingly, the strong coupling expansion also gives confinement with a U(1) gauge group. As this is the gauge group of electrodynamics, it is essential that the lattice system undergo a phase transition into an unconfined phase of photon and electron. As quantum electrodynamics is the prototype gauge theory, the viability of Wilson's formulation depends on its applicability here. Guth has recently given rigorous arguments that the pure (U(1) lattice gauge theory will indeed possess distinct strong and weak coupling phases.[5]

Lattice gauge theories are an example of a class of systems discovered by Wegner[6] where no local order parameter distinguishes the various phases. Wilson has circumvented this problem by defining a non-local correlation function, the Wilson loop.[3] The asymptotic behavior of large loops is directly related to the phenomenon of confinement. Thus, theoretical interest is concentrated on the study of these gauge invariant quantities.

An intriguing approximate recursion relation for lattice gauge theory has been presented by Migdal and Kadanoff.[7] With certain approximations, the theory on a given lattice is related to the theory with a multiple of this lattice spacing. The remarkable feature of this relation is that it exhibits a close analogy between gauge theories in d dimensions and nearest neighbor spin systems in d/2 dimensions. This suggests that four dimensional gauge models should exhibit similar phase structure to two dimensional statistical mechanical systems for which there exists a substantial body of lore and exact results. In particular, the two dimensional model which corresponds to the four dimensional SU(3) gauge theory of the strong interactions is a generalization of the Heisenberg model and in two dimensions should have only one phase. This has been widely touted as evidence for the absence of extraneous phase transitions in the gauge theory and thus the coexistence of asymptotic freedom and confinement. In contrast, the two dimensional system corresponding to four-dimensional lattice quantum electrodynamics is the planar or XY model and does indeed possess two distinct phases.

Being only an approximation, the Migdal relations may misidentify the nature of transition. The most striking example is the case of Z_2 gauge theory in four dimensions which has a clear first order transition[8] whereas the corresponding two dimensional spin system is the Ising model, which possesses a second order transition. Despite these uncertainties, the Migdal relations represent the strongest argument besides Monte Carlo numerical work for confinement in asymptotically free gauge theories.

Although the Monte Carlo approach to simulating statistical systems is quite old,[9] only recently did Wilson propose its application to the study of gauge fields.[10] The goal of this approach is to generate in

a stochastic manner a set of field configurations which are representative of the dominant contribution to the path integral defining the quantum theory. By measuring various correlation functions in this set, one obtains an approximation to the true Green's function of the theory. The error in this measurement can be estimated from the fluctuations of the measured function from one configuration to another. In these lectures, I will endeavor to show how Monte Carlo techniques have yielded strong support to the above picture of phase transitions in lattice gauge theory.

II. The Wilson action and renormalization

Wilson's elegant lattice formulation[3] is based on the concept that a gauge field represents a theory of non-integrable phase factors.[12] When a material particle traverses some world line C in space time, its interaction with the electromagnetic field appears as a phase factor in its wave function

$$\psi \to \exp\left(ig\int_C A_\mu \, dx_\mu\right)\psi \qquad (2.1)$$

where g is the particles charge and A_μ is the vector potential. The dynamics of the matter field follow from a path integral over all possible world lines. For a non-Abelian theory the phase factor becomes a matrix belonging to the gauge group and the integral in eg. (2.1) is defined with a "path ordering" prescription.

On a hypercubical lattice, we now approximate an arbitrary world line with a sequence of steps between neighboring lattice sites. The above phase factor then becomes the product of phases associated with each step of the path. This leads to using as variables an element U_{ij}, from the gauge group, associated with every nearest neighbor pair of sites $\{i,j\}$ on the lattice. In the gauge theory of the strong interaction these are all elements of SU(3). Traversing a link in the opposite direction gives the inverse element

$$U_{ij} = (U_{ji})^{-1} \qquad (2.2)$$

The path integral

$$Z = \int \prod_{i,j} dU_{ij} \; e^{-\beta S(U)} \qquad (2.3)$$

defines the quantum theory. Here the integral includes all independent link variables and uses the invariant group measure. The action S is a

sum over all elementary squares or "plaquettes" in the lattice

$$S(U) = \sum_{\square} S_{\square} \tag{2.4}$$

where $$S_{\square} = 1 - \frac{1}{N} \mathrm{Re}\ \mathrm{Tr}(U_{ij}\ U_{jk}\ U_{kl}\ U_{li}) \tag{2.5}$$

Here i, j, k, and l label sites circulating about the square and N is the dimension of the matrices U. To connect this action with the continuum theory, identify

$$U_{ij} = \exp\left(-ig_o(x^i - x^j)_\mu A_\mu \left(\frac{x^i + x^j}{2}\right) \right) \tag{2.6}$$

where g_o is the bare coupling constant, x^i are the coordinates of the site i, and A_μ is the gauge potential regarded as an element of the lie algebra of the group. If A_μ is smooth and can be Taylor expanded about the center of the plaquette, a little algebra gives

$$S_{\square} = \frac{1}{4N} g_o{}^2\ a^4\ \mathrm{Tr}(F_{\mu\nu}F_{\mu\nu} + F_{\nu\mu}F_{\nu\mu}) \tag{2.7}$$

Here μ and ν are not summed over and determine the plane of the square, a is the lattice spacing, and $F_{\mu\nu}$ is the usual field strength tensor

$$F_{\mu\nu} = \partial_\mu A_\nu - \partial_\nu A_\mu + ig_o\ [A_\mu, A_\nu] \tag{2.8}$$

Combining the a^4 in eq. 2-7 with the sum over plaquettes in eq. 2.4 gives a four dimensional integral as the lattice spacing goes to zero. Consequently, we conclude that

$$S(U) \to \int d^4x\ \tfrac{1}{2}\mathrm{Tr}(F_{\mu\nu}F_{\mu\nu}) \tag{2.9}$$

with

$$\beta = \frac{2N}{g_o{}^2} \tag{2.10}$$

For the Abelian gauge group the continuum limit is a free theory; however, on the lattice a residual interaction survives. For this model the conventional normalization is

$$\beta_{U(1)} = \frac{1}{g_o{}^2} \tag{2.11}$$

in contrast to eq.(2.10).

The parameter g_o is the bare coupling constant with the lattice in place. To take the continuum limit of the quantum theory, one takes a to zero while continually adjusting g_o to keep some physical parameter fixed. The particular parameter chosen determines the renormalization scheme. Given such a scheme, g_o is a function of a and one can define a Gell-Mann-Low function as

$$\gamma(g_o) = a \frac{\partial g_o(a)}{\partial a} \tag{2.12}$$

For small bare coupling $\gamma(g_o)$ can be expanded perturbatively

$$\gamma(g_o) = \gamma_o g_o^3 + \gamma_1 g_o^5 + O(g_o^7) \tag{2.13}$$

These first two coefficients are independent of renormalization scheme and for SU(N) are[13]

$$\gamma_o = \frac{11}{3}\left(\frac{N}{16\pi^2}\right) \tag{2.14}$$

$$\gamma_1 = \frac{34}{3}\left(\frac{N}{16\pi^2}\right)^2 \tag{2.15}$$

Eqs. 2.12 - 2.15 can be integrated to give

$$g_o^2(a) = \frac{1}{\gamma_o \ell n\left(\frac{1}{\Lambda_o{}^2 a^2}\right) + \left(\frac{\gamma_1}{\gamma_o}\right) \ell n\left[\ell n\left(\frac{1}{\Lambda_o{}^2 a^2}\right)\right] + O(g_o^2)} \tag{2.16}$$

Where Λ_o is an integration constant. This equation displays the phenomenon of asymptotic freedom; the bare coupling goes to zero logarithmically with the lattice spacing in the continuum limit. Eq. 2.16 can be rewritten in a

form defining Λ_o

$$\Lambda_o = \lim_{a\to o} \frac{1}{a} [\gamma_o g_o^2(a)]^{(-\gamma_1/2\gamma_o^2)} \exp[\frac{-1}{2\gamma_o g_o^2(a)}] \qquad (2.17)$$

In a study of confinement, a natural physical quantity to use for renormalization purposes is the string tension. This quantity can be extracted from a study of Wilson loops. For a closed contour C of links in the lattice, the Wilson loop is defined as

$$W(C) = < \frac{1}{N} \mathrm{Tr} \left(\prod_C U\right)_{p.o.} > \qquad (2.18)$$

Here P.O. represents "path ordering"; that is, the U_{ij} are ordered and oriented as they are encountered in circulating about the contour. The simplest non-trivial loop arises when C is a single plaquette, in which case

$$W(\square) = 1 - < S_\square > \qquad (2.19)$$

The expectation value in these equations is in the sense of the integration of eq. 2.3.

If for large separations the interaction energy of two static sources in the fundamental representation of the gauge group increases linearly with distance, then one expects for large contours

$$\ln W(c) = -KA(C) + O[p(C)] \qquad (2.20)$$

where A(C) is the minimal area enclosed by C and p(C) is the contour perimeter. the string tension K is precisely the coefficient of the linear part of the static quark-antiquark potential. Measuring A in physical units, it equals the lattice spacing squared times $N_\square(C)$, the minimum number of plaquettes

forming a surface bounded by C. Thus we write

$$\ell n\, W(C) = -(a^2K)N\,(C) + O[p(C)] \tag{2.21}$$

By measuring the exponential falloff of W(C) with N , we effectively measure the dimensionless product a^2K as a function of the bare coupling g_o.

Assuming the linear potential survives the continuum limit, then the string tension is a physical quantity which can be held fixed as a renormalization prescription. Eq. 2.17 then tells us how a^2K must behave for small a

$$a^2K \underset{a\to o}{\longrightarrow} \frac{K}{\Lambda_o^2}\,(\gamma_o g_o^2)^{(-\gamma_1/\gamma_o^2)}\,\exp(-\frac{1}{\gamma_o g_o^2}) \tag{2.22}$$

One goal of the Monte Carlo work has been to verify eq. 2.22 and thereby measure the ratio $K/\Lambda_o{}^2$. This represents a true non-perturbative calculation relating the long distance forces represented in K and the asymptotically free short distance behavior characterized by Λ_0.

III. The Monte Carlo approach

The basic goal of a Monte Carlo procedure for a system of degrees of freedom U_{ij} is to stochastically generate a sequence of configurations C_k such that asymptotically the probability density of any particlar configuration is proportional to the Boltzmann factor

$$P(C) \sim e^{-\beta S(C)} \tag{3.1}$$

Expectation values of functions of the U_{ij} in this sequence are then identified with the corresponding Green's function obtained from the path integral.

In practice, most Monte Carlo algorithms are based on a principle of detailed balance.[11] Let $P(C \to C')$ denote the probability that a given configuration c in the sequence yields C' as the next configuration. If P satisfies

$$P(C \to C')e^{-\beta S(C)} = P(C' \to C)e^{-\beta S(C')} \tag{3.2}$$

it is straightforward to define a norm between ensembles of configurations such that application of this Monte Carlo procedure will reduce the distance between any given ensemble and the equilibrium ensemble satisfying eq. 3.1. If the algorithm has eventual access to any configuration, then ultimately eq.3.1 will be approached.

This detailed balance condition is rather general in that many different functions $P(C \to C')$ can satisfy eq. 3.2. For simplicity, usually only one degree of freedom U_{ij} is varied at a time. The most intuitive algorithm is to replace the given U_{ij} with a new value chosen randomly from all allowed values with a weight proportional to the exponentiated action in eq. 3.1, but with all other U_{ij} held fixed at their current values.[15,16] Physically,

this is equivalent to placing a heat bath at inverse temperature β in contact with the variable in question. This procedure is then repeated on all the variables in the system and then the algorithm is iterated.

In processing a given variable, this heat bath method reduces the distance of an ensemble from equilibrium by the most of any algorithm working on that variable. This follows because repeated application of any other algorithm to a single variable eventually approaches the heat bath method. Unfortunately, the generation of an appropriately weighted new variable may be complicated and time consuming. Thus, considerably computationally simpler algorithms satisfying eq. 2. have been devised. Nonetheless, for variables in relatively simple manifolds, such as U(1) or SU(2), implementation of a heat bath algorithm can result in considerable savings of computer time. This is particularly the case in gauge theories, where merely combining the interacting neighbor variables is the bulk of the computation. Except for SU(N) with $N \geq 3$, where I have used a technique similar to Wilson, I have always used the heat bath method. In appendix A is a listing of a Fortran program for a heat bath simulation of SU(2) lattice gauge theory.

Figure 3.1 illustrates the convergence of this Monte Carlo procedure on SU(2) lattice gauge theory. The value $\beta = 2.3$ is selected as representative of the slowest convergence in this model. The figure shows the average plaquette, or internal energy

$$P = \langle 1 - \tfrac{1}{2}\mathrm{Tr} \prod_{\square} (U_{ij}) \rangle , \tag{3.3}$$

as a function of number of iteration for a total of 30 iterations. One iteration represents application of the heat bath algorithm once to each link in the entire lattice. Runs are shown where the initial lattice was totally ordered, $U_{ij} = 1$, and also totally disordered, each U_{ij} picked

from the gauge group uniformly with the invariant group measure. Runs are shown for various lattices of size from 4^4 to 10^4. Note that the convergence rate is essentially independent of lattice size, only the thermal fluctuations grow on the smaller lattices.

Figure 3.2 shows the evolution from an ordered state on an 8^4 lattice for several values of β. Note the absence of any dramatic β dependence of the convergence rate; a slight slowing occurring in the range $\beta = 2 - 2.4$. This shows that the method is not tied to either the high or low temperature regimes.

These first two figures show the situation for a non-Abelian theory where no phase transitions are expected. When a transition does occur, convergence can be considerably worse. Figure 3.3 shows a run with an ordered start for the gauge group Z_2, i.e. each $U_{ij} \epsilon \{\pm 1\}$. This system is known to have a phase transition at $\beta_c = \frac{1}{2}\ell n(1+\sqrt{2}) = .44...$ For this figure we work at a value of β just below this transition, $\beta = .425$. Thus, we are attempting to heat the system through the phase transition. Note that convergence now takes several hundred iterations and that the system appears to pass through a metastable state. In figure 3.4 we show runs with ordered and disordered starts, both with $\beta = \beta_c$. Here there is no tendency for the runs to come together, and the system has two distinct stable phases. This is indicative of a first order transition in this model.

As convergence is poor near a phase transition and good elsewhere, a rapid thermal cycle can quickly reveal regions of structure is a given model. In figure 3.5 we show such thermal cycles on SU(2) gauge theory in 4 and 5 space-time dimensions and for the U(1) = SO(2) theory in 4 dimensions.[18] Each point was obtained by heating or cooling the system on the order of

twenty iterations. Phase transitions are suggested in those regions where the heating and cooling curves do not agree. Such "hysteresis" phenomena are clear in the 5 dimensional SU(2) and the four dimensional U(1) models. More detailed analysis by Lautrup and Nauenberg[19] has presented evidence that the U(1) transition is second order, while analysis of our own suggests a first order transition in the 5 dimensional SU(2) case. This clear transition in 5 dimensions shows the critical nature of 4 dimensions where no strong structure is seen for SU(2).[20]

Once a lattice is in reasonable equilibrium, it is all stored in the computer memory and any desired correlation function can be measured. In figure 3.6 we show the expectation values for square Wilson loops at $\beta = 3$ and as a function of lattice size. These loops lie in a fundamental plane of the lattice and are up to six links on a side. Each measurement is an average over all translations and rotations of the loops. The error bars represent the standard deviation of the loops over a sequence of five iterations after attaining equilibrium. As expected, larger loops show the finite size effects most strongly. In general, loops of up to half the lattice size appear to have stabilized.

To extract an area law dependence of the loops, it is convenient to construct the quantities[12]

$$\chi(I,J) = -\ln\left[\frac{W(I,J)W(I-1,J-1)}{W(I,J-1)W(I-1,J)}\right] \tag{3.4}$$

Here W(I,J) is the rectangular loop of dimensions I x J in lattice units. In this combination overall constant factors and perimiter behavior will cancel. In a regime where the loops are dominated by an area law

$$W(I,J) \sim e^{-KA} \tag{3.5}$$

where $A = a^2IJ$ is the loop area, χ directly measures the string tension

$$\chi \to a^2K \tag{3.6}$$

This happens whenever I and J are large or when the bare coupling is large. However, in the weak coupling limit for fixed I and J, χ should have a perturbative expansion

$$\chi(I,J) = a_1 g_o^2 + O(g_o^4) \tag{3.7}$$

In particular, a simple calculation gives

$$\chi(1,1) \underset{g_o^2 \to o}{} \begin{cases} \frac{3}{16} g_o^2 & SU(2) \\ \frac{1}{3} g_o^2 & SU(3) \end{cases} \tag{3.8}$$

This power behavior is radically different from the essential singularity in eq. (2.22) expected for the right hadn side of eq. (3.6).

To summarize, for strong coupling we expect all $\chi(I,J)$ to approach the coefficient of the area law, but as g_o^2 is reduced the smaller values of I and J should begin to deviate from the larger area. Thus, we expect all $\chi(I,J)$ to form an envelope along the true value of a^2K as a function of g_o^2. In figures 3.7 and 3.8 I plot the values of $\chi(I,J)$ for the gauge groups SU(2) and SU(3). The error bars represent the standard deviation of the mean taken from an ensemble of five configurations. On these graphs I show the strong coupling limits

$$\chi(I,J) = \begin{cases} \ln(g_o^2) + O(g^{-4}) & SU(2) \\ \ln(3g_o^2) + O(g^{-2}) & SU(3) \end{cases} \tag{3.9}$$

as well as the weak coupling behavior for a^2K from eq. 2.2. The weak coupling bands correspond to

$$\frac{\Lambda_o}{\sqrt{K}} = \begin{cases} (1.3 \pm 0.2) \times 10^{-2} & SU(2) \\ (5.0 \pm 1.5) \times 10^{-3} & SU(3) \end{cases} \tag{3.10}$$

Hasenfratz and Hasenfratz[22] have done a lengthy perturbative calculation relating the lattice Λ_o to a more conventional scale Λ_{MOM} defined by the three gluon vertex in Feynman gauge at a given scale in momentum space. They find

$$\Lambda^{MOM} = \begin{cases} 57.5\ \Lambda_o & SU(2) \\ 83.5\ \Lambda_o & SU(3) \end{cases} \tag{3.11}$$

Combining the previous equation relates Λ_{MOM} to the confining linear potential

$$\frac{\Lambda^{MOM}}{\sqrt{K}} = \begin{cases} 0.75 \pm 0.12 & SU(2) \\ 0.42 \pm 0.13 & SU(3) \end{cases} \tag{3.12}$$

If we accept the string model connection between K and the Regge slope

$$K = \frac{1}{2\pi\alpha'} \tag{3.13}$$

and use $\alpha' = 1.0\ (GeV)^{-2}$, then we conclude for SU(3)

$$\Lambda^{MOM} = 170 \pm 50\ MeV \tag{3.14}$$

This number is somewhat below the currently most popular phenomenological value of $\sim$800 MeV. Some difference is expected because all effects of virtual quarks are absent from our calculation.

IV. Renormalization group studies[23]

The goal of renormalization is to remove ultraviolet divergences from quantum field theory. The basic coupling parameters become functions of an ultraviolet cutoff in such a manner that physical quantities have a finite limit as the cutoff is removed. The pure gauge theories discussed here have only one bare coupling parameter g_o. A general physical observable P is a function of g_o, the cutoff of length a, and the scale r on which P is measured

$$P = P(r,a,g_o(a)) \tag{4.1}$$

Here we explicitly indicate the cutoff dependence of g_o. For simplicity we assume P is dimensionless; if not, just multiply by enough factors of r to make it so.

As the cutoff a becomes small and we approach the continuum limit, P should approach its physical value. Considering a factor of two change in cutoff, we expect

$$P(r,\tfrac{a}{2},g_o(\tfrac{a}{2})) = P(r,a,g_o(a)) + O(a^2) \tag{4.2}$$

In general there are two classes of dimensional parameters which set the scale for the $O(a^2)$ corrections in this equation. First is the scale r used to define P. Second, there are dimensional parameters characterizing the continuum theory. In particular, regardless of the value of r, we expect corrections in eq. 2.2 of order a^2m^2 where m is a typical mass in the physical spectrum. One should not use the lattice theory for phenomenology when the cutoff is larger than a typical hadronic size.

If one adopts the renormalization scheme of holding $P(r,a,g_o(a))$ fixed for some given r, then at that scale there are by definition no $O(a^2)$

corrections in eq. 4.2. However, we will be varying r and thus these corrections are expected to enter. Indeed, as we will be working on a lattice of only 10^4 sites, these corrections could be substantial. Nonetheless, we proceed with optimism and neglect these terms.

Since P is dimensionless, we can scale a factor of 2 from both r and a to obtain

$$P\left[2r,a,g_o\left(\frac{a}{2}\right)\right] = P\left[r,a,g_o(a)\right] \tag{4.3}$$

where we neglect the $O(a^2)$corrections. We now iterate and take r to $2^{-n}r$ to give

$$P\left[2r,a,g_o\left(\frac{a}{2^{n+1}}\right)\right] = P\left[r,a,g_o\left(\frac{a}{2^n}\right)\right] \tag{4.4}$$

Thus a measurement of P at two scales relates the bare coupling at two values of cutoff.

Eq. 4.4 has a simple graphical interpretation. Assume that for some given values of r and a we use some techniques such as Monte Carlo to evaluate

$$F(g_o) \equiv P(r,a,g_o) \tag{4.5}$$

$$G(g_o) \equiv P(2r,a,g_o) \tag{4.6}$$

Suppose that at scale r and in the continuum limit P has the value P_o.

$$\lim_{a\to o} P\left[r,a,g_o(a)\right] = P_o \tag{4.7}$$

Then on a graph of $F(g_o)$ versus g_o, we can define $g_o(a)$ as the value of g_o where

$$F\left[g_o(a)\right] = P_o \tag{4.8}$$

From eq. 4.3 we now find $g_o\left(\frac{a}{2}\right)$

$$G\left[g_o\left(\frac{a}{2}\right)\right] = P_o \tag{4.9}$$

we then define P_1 by

$$P_1 = F\left[g_o\left(\frac{a}{2}\right)\right] \tag{4.10}$$

Iterating by using eq. 4.4 gives

$$G\left[g_o\left(\frac{a}{2n}\right)\right] = P_{n-1} \tag{4.11}$$

$$P_n = F\left[g_o\left(\frac{a}{2n}\right)\right] \tag{4.12}$$

This sequence of steps is illustrated in fig. 4.1 for an asymptotically free theory with $g_o(0) = 0$. Fig. 4.2 shows the situation with a renormalization group fixed point $g_o(0) = g_F$ which satisfies

$$F(g_F) = G(g_F) \tag{4.13}$$

We wish to carry out the above construction for SU(2) and U(1) lattice gauge theory and use Monte Carlo techniques to evaluate F and G. As Wilson loops are the most easily measured correlation functions, we would like to use them to construct P. Unfortunately the bare Wilson loop has ultraviolet divergences in the continuum limit. These divergences are of a rather trivial nature, being due to the self energies of the point-like nature of the contour. We assume that if this divergence, proportional to the loop perimeter, is removed, and the coupling constant appropriately renormalized, then the loops have finite continuum limits. The easiest way for us to do this is to take ratios of loops with the same perimeter but different shapes. Thus motivated, we define

$$F(g_o) = 1 - \frac{W(2,2)W(1,1)}{(W(2,1))^2} \tag{4.14}$$

$$G(g_o) = 1 - \frac{W(4,4)W(2,2)}{(W(4,2))^2} \tag{4.15}$$

The constant is added so that these quantities are proportional to g_o^2 for small g_o. In these equations we have taken r = 2a and r = 4a in the general physical ratio

$$P(r,a,g_o) = 1 - \frac{W\left(\frac{r}{a},\frac{r}{a}\right) W\left(\frac{r}{2a},\frac{r}{2a}\right)}{\left[W\left(\frac{r}{a},\frac{r}{2a}\right)\right]^2} \tag{4.16}$$

In fig. 4.3 we show these quantities F and G for the gauge group SU(2). Note that F always lies below G suggesting a picture like that in fig. 4.1. There is no evidence for a fixed point other than at $g_o = 0$. The figure also shows the strong coupling behaviors expected for F and G. For $g_o^2 > 2$ the numerical results approximate that behavior, consequently no further structure is expected.

In fig. 4.4 we show these functions for the U(1) theory. In striking contrast to the SU(2) case, at $g_o^2 \approx 1$ the function F and G meet. A crossover is suggested but may not be statistically significant. When g_o^2 is substantially below g_F^2 the functions are equal within errors. This indicates a scale invariant theory dominated by massless photons.

As we are changing scales by a factor of two, asymptotic freedom tells us

$$\frac{1}{g_o^2\left(\frac{a}{2}\right)} = \frac{1}{g_o^2(a)} + 2\gamma_o \ell n 2 + O(g_o^2) \tag{4.17}$$

where γ_o is given in eq. 2.14. Thus we expect for small g_o^2 with the group SU(2)

$$F(g_o) = G\left[\left(\frac{1}{g_o^2} - \frac{11}{12\pi^2}\ell n 2\right)^{-\frac{1}{2}}\right] \tag{4.18}$$

In figure 4.5 we plot our points for F along with those for G with the shift

indicated in this equation. This agreement is rather astonishing in the light of the neglected $0\left(\frac{a^2}{r^2}\right)$ correction.

The function P in eq. 4.16 can be expanded perturbatively. To lowest order for SU(2)

$$P(r,a,g_o) = p_1 g^2(r) + 0(g^4) + 0\left(\frac{a^2}{r^2}\, g^2\right) \tag{4.19}$$

where

$$p_1 = \frac{1}{4\pi^2}\left(8 \arctan 2 + 2 \arctan \tfrac{1}{2} - 2\pi - 4\ell n \frac{5}{4}\right)$$

$$= 0.066079788... \tag{4.20}$$

Here $g^2(r)$ is any coupling defined at scale r. Indeed, the specification of $g^2(r)$ is sufficiently free that we can define

$$g^2(r) = \frac{1}{p_1} \lim_{a\to o} P\left[r,a,g_o(a)\right] \tag{4.21}$$

Neglecting finite cutoff corrections, the function F then measures $g^2(r)$ at $r = 2a$. Any coupling defines an asymptotic freedom scale Λ in analogy to eq. 2.16

$$g^2(r) = \frac{1}{\gamma_o \ell n\left(\frac{1}{\Lambda^2 r^2}\right) + \frac{\gamma_1}{\gamma_o}\, \ell n\left[\ell n\left(\frac{1}{\Lambda^2 r^2}\right)\right] + 0(g^2)} \tag{4.22}$$

For small coupling we expect

$$\frac{1}{g_o^2(a)} = \frac{1}{g^2(2a)} + 2\gamma_o \ell n\left(\frac{2\Lambda}{\Lambda_o}\right) + 0(g^{-4}) \tag{4.23}$$

In fig. 4.6 we plot these inverse couplings against each other. Note that at large inverse charges the graph approaches a straight line as predicted by eq. 4.2 . The unit slope of this line demonstrates that the a^2/r^2 corrections are remarkably small. From the intercept of this line we obtain

$$2\beta_o \ell n \left(\frac{2\Lambda}{\Lambda_o}\right) = 0.35 \tag{4.24}$$

or

$$\Lambda = 22\Lambda_o \tag{4.25}$$

This number is in principle calculable with a one loop perturbative analysis.

Appendix A

Here I give a simple program for Monte Carlo simulation of SU(2) lattice gauge theory in four dimensions. It is in Fortran although in a few places several statements are placed on one line using the "$" symbol. The method for generating the new group elements is described in Ref. (16).

```
      PROGRAM LATTICE(OUTPUT)
      COMMON/VAR/B,ISIZE,MDOWN(10),MUP(10),IPOWER(5),APQ
      COMMON/VAR1/U11(40000)
      COMMON/VAR2/U12(40000)
      LEVEL2,U11,U12
      COMPLEX U11,U12
C  LATTICE=ISIZE*ISIZE*ISIZE*ISIZE
C  INVERSE TEMPERATURE = B
C  SUBROUTINE MONTE(I) GIVES I MONTE CARLO ITERATIONS PER LINK
C MUP AND MDOWN SHIFT N PERIODICALLY IN ISIZE
C DO NOT RUN WITH B=0
      ISIZE=10
      B=2.6
      DO 5 N=1,ISIZE
      MUP(N)=MOD(N,ISIZE)+1
5     MDOWN(N)=MOD(N-2+ISIZE,ISIZE)+1
      DO 6 N=1,5
6     IPOWER(N)=ISIZE**(N-1)
      MF=4*ISIZE**4
      DO 67 M=1,MF
      U11(M)=1
67    U12(M)=0
      CALL MONTE(30)
      STOP $ END


      SUBROUTINE MONTE(ITER)
      COMMON/VAR/B,ISIZE,MDOWN(10),MUP(10),IPOWER(5),APQ
      COMMON/VAR1/U11(40000)
      COMMON/VAR2/U12(40000)
      LEVEL2,U11,U12
      COMPLEX U11,U12,UINT11,UINT12,NEW11,NEW12
      COMPLEX A12S1,A26S1,A65S1,A13S1,A34S1,A45S1,A126S1,A134S1
      COMPLEX A12S2,A26S2,A65S2,A13S2,A34S2,A45S2,A126S2,A134S2
      INTEGER X(4)
      PRINT*,ITER," ITERATION(S)"
      TEMP=1/B
      BX2=B*2
      DO 51 NIT=1,ITER
      SUM=0
```

```
C SITE LOOPS
      MA=-IPOWER(2)-IPOWER(3)-IPOWER(4)-IPOWER(5)
      DO 50 IS=1,ISIZE $ X(4)=IS $ MB=MA+IS*IPOWER(4)
      DO 50 JS=1,ISIZE $ X(3)=JS $ MC=MB+JS*IPOWER(3)
      DO 50 KS=1,ISIZE $ X(2)=KS $ MD=MC+KS*IPOWER(2)
      DO 50 LS=1,ISIZE $ X(1)=LS $ M1=MD+LS
C SELECT LINK
      DO 50 I1=1,4
      UINT11=UINT12=0
C SITES LABELED:   2--6
C                  1--5
C                  3--4
C LOCATE NEXT SITE IN I1 DIRECTION
      M45=IPOWER(I1)*(MUP(X(I1))-X(I1))
      M5=M1+M45
      I1IP5=I1*IPOWER(5)
      L15=M1+I1IP5
C LOOP OVER PLANES CONTAINING LINK
      DO 1 I2=1,4
      IF (I1.EQ.I2) GO TO 1
C LOCATE NEIGHBORING SITES AND LINKS
      M2=M1+IPOWER(I2)*(MUP(X(I2))-X(I2))
      M3=M1+IPOWER(I2)*(MDOWN(X(I2))-X(I2))
      M4=M3+M45
      I2IP5=I2*IPOWER(5)
      L12=M1+I2IP5
      L31=M3+I2IP5
      L34=M3+I1IP5
      L45=M4+I2IP5
      L56=M5+I2IP5
      L26=M2+I1IP5
C OBTAIN INTERACTING SPINS
      A12S1=U11(L12) $ A12S2=U12(L12)
      A26S1=U11(L26) $ A26S2=U12(L26)
      A34S1=U11(L34) $ A34S2=U12(L34)
      A45S1=U11(L45) $ A45S2=U12(L45)
      A65S1=CONJG(U11(L56)) $ A65S2=-U12(L56)
      A13S1=CONJG(U11(L31)) $ A13S2=-U12(L31)
C MULTIPLY INTERACTING SPINS
      A126S1=A12S1*A26S1-A12S2*CONJG(A26S2)
      A126S2=A12S1*A26S2+A12S2*CONJG(A26S1)
      A134S1=A13S1*A34S1-A13S2*CONJG(A34S2)
      A134S2=A13S1*A34S2+A13S2*CONJG(A34S1)
      UINT11=UINT11+A126S1*A65S1
     C   -A126S2*CONJG(A65S2)
     C   +A134S1*A45S1
     C   -A134S2*CONJG(A45S2)
      UINT12=UINT12+A126S1*A65S2
     C   +A126S2*CONJG(A65S1)
     C   +A134S1*A45S2
     C   +A134S2*CONJG(A45S1)
```

```
1       CONTINUE
C SELECT NEW GROUP ELEMENT
        UMAG=SQRT(REAL(UINT11)**2+AIMAG(UINT11)**2
       C  +REAL(UINT12)**2+AIMAG(UINT12)**2)
        UMAGIN=1/UMAG
        TEFF=UMAGIN*TEMP
        OME2B=AMIN1(1.,BX2*UMAG)
6       A0=1.+ALOG(1.-OME2B*RANF(0))*TEFF
        RAD=1-A0**2
        IF (RANF(0)**2.GT.RAD) GO TO 6
        A3=SQRT(RAD)*(2*RANF(0)-1.)
8       A1=RANF(0)-.5 $ A2=RANF(0)-.5
        RAD=A1**2+A2**2
        IF (RAD.GT..25) GO TO 8
        NEW11=CMPLX(A0,A3)*UMAGIN
        NEW12=CMPLX(A2,A1)*(UMAGIN*SQRT((1.-A0**2-A3**2)/RAD))
        U11(L15)=NEW11*UINT11-NEW12*CONJG(UINT12)
        U12(L15)=NEW11*UINT12+NEW12*CONJG(UINT11)
C PUT NEW ACTION INTO SUM
50      SUM=SUM+A0*UMAG
        APQ=1.-SUM/(24.*ISIZE**4)
51      PRINT100,ISIZE,B,APQ
100     FORMAT("      SIZE=",I2,"     GROUP=SU(2)",
       C  "    B=",F6.4,"    AV.PQ.=",F6.4)
        RETURN
        END
```

This program runs on a CDC 7600 in just under 200 seconds. The resulting output is:

```
30 ITERATION(S)
 SIZE=10    GROUP=SU(2)    B=2.6000    AV.PQ.= .2025
 SIZE=10    GROUP=SU(2)    B=2.6000    AV.PQ.= .2921
 SIZE=10    GROUP=SU(2)    B=2.6000    AV.PQ.= .3138
 SIZE=10    GROUP=SU(2)    B=2.6000    AV.PQ.= .3242
 SIZE=10    GROUP=SU(2)    B=2.6000    AV.PQ.= .3246
 SIZE=10    GROUP=SU(2)    B=2.6000    AV.PQ.= .3274
 SIZE=10    GROUP=SU(2)    B=2.6000    AV.PQ.= .3292
 SIZE=10    GROUP=SU(2)    B=2.6000    AV.PQ.= .3273
 SIZE=10    GROUP=SU(2)    B=2.6000    AV.PQ.= .3271
 SIZE=10    GROUP=SU(2)    B=2.6000    AV.PQ.= .3260
 SIZE=10    GROUP=SU(2)    B=2.6000    AV.PQ.= .3265
 SIZE=10    GROUP=SU(2)    B=2.6000    AV.PQ.= .3282
 SIZE=10    GROUP=SU(2)    B=2.6000    AV.PQ.= .3303
 SIZE=10    GROUP=SU(2)    B=2.6000    AV.PQ.= .3304
 SIZE=10    GROUP=SU(2)    B=2.6000    AV.PQ.= .3290
 SIZE=10    GROUP=SU(2)    B=2.6000    AV.PQ.= .3275
 SIZE=10    GROUP=SU(2)    B=2.6000    AV.PQ.= .3302
 SIZE=10    GROUP=SU(2)    B=2.6000    AV.PQ.= .3295
 SIZE=10    GROUP=SU(2)    B=2.6000    AV.PQ.= .3295
 SIZE=10    GROUP=SU(2)    B=2.6000    AV.PQ.= .3298
 SIZE=10    GROUP=SU(2)    B=2.6000    AV.PQ.= .3283
 SIZE=10    GROUP=SU(2)    B=2.6000    AV.PQ.= .3305
 SIZE=10    GROUP=SU(2)    B=2.6000    AV.PQ.= .3324
 SIZE=10    GROUP=SU(2)    B=2.6000    AV.PQ.= .3314
 SIZE=10    GROUP=SU(2)    B=2.6000    AV.PQ.= .3302
 SIZE=10    GROUP=SU(2)    B=2.6000    AV.PQ.= .3301
 SIZE=10    GROUP=SU(2)    B=2.6000    AV.PQ.= .3298
 SIZE=10    GROUP=SU(2)    B=2.6000    AV.PQ.= .3305
 SIZE=10    GROUP=SU(2)    B=2.6000    AV.PQ.= .3299
 SIZE=10    GROUP=SU(2)    B=2.6000    AV.PQ.= .3293
```

References

1. W. Marciano and H. Pagels, Phys. Reports 36C, 139 (1978).
2. C. G. Callan, R. F. Dashen, and D. J. Gross, Phys. Rev. D19, 1826 (1979).
3. K. Wilson, Phys. Rev. D10, 2445 (1974).
4. R. Balian, J. M. Drouffe, and C. Itzykson, Phys. Rev. D10, 3376 (1974; 11, 2098 (1975); 11, 2104 (1975).
5. A. Guth, Phys. Rev. D21, 2291 (1980).
6. F. Wegner, J. Math. Phys. 12, 2259 (1971).
7. A. A. Migdal, ZH. Eksp. Teor. Fiz. 69, 810 (1975); 69, 1457 (1975) {Sov. Phys. - JFTP 42, 413 (1975); 42, 743 (1975)}; L. P. Kadanoff, Rev. Mod. Phys. 49, 267 (1977).
8. M. Creutz, L. Jacobs, and C. Rebbi, Phys. Rev. Lett. 42, 1390 (1979).
9. N. Metropolis, A. W. Rosenbluth, M. N. Rosenbluth, A. H. Teller, and E. Teller, J. Chem. Phys. 21, 1087 (1953).
10. K. Wilson, in New Developments in Quantum Field Theory and Statistical Mechanics: Cargese 1976, Edited by M. Levy and P. Mitter (Plenum Press, New York, 1977).
11. K. Binder, in Phase Transitions and Critical Phenomena, edited by C. Domb and M. S. Green (Academic, New York, 1976), Vol. 5B.
12. S. Mandelstam, Ann. Phys. 19, 1 (1962); C. N. Yang, Phys. Rev. Lett. 33, 445 (1975).
13. W. E. Caswell, Phys. Rev. Lett. 33, 244 (1974); D. R. T. Jones, Nucl. Phys. B75, 531 (1974).
14. J. B. Kogut, R. B. Pearson, and J. Shigemitsu, Phys. Rev. Lett. 43, 484 (1979).

15. C.-P. Yang, Proceedings of Symposia in Applied Mathematics, Vol. XV, Amer. Math Soc. (1963).

16. M. Creutz, Phys. Rev. D21, 2308 (1980).

17. K. G. Wilson, preprint (1979).

18. M. Creutz, Phys. Rev. Lett. 43, 553 (1979).

19. B. Lautrup and M. Nauenberg, Phys. Lett. 95B, 63 (1980).

20. The SU(2) model in four dimensions does show a peculiar structure in its specific heat. See B. Lautrup and M. Nauenberg, Phys. Rev. Lett. 45, 1755 (1980). For a similar analysis of SU(3) see R. C. Edgar, L. McCrossen and K. J. M. Moriarty, preprint (1980).

21. M. Creutz, Phys. Rev. Lett. 45, 313 (1980).

22. A. Hasenfratz and P. Hasenfratz, Phys. Lett. 93B, 165 (1980).

23. This section is a condensed version of M. Creutz, BNL preprint 28736 (1980).

Figure Captions

Fig. 3.1. The average plaquette for SU(2) gauge theory at $\beta = 2.3$ as a function of number of Monte Carlo iterations.

Fig. 3.2. The evolution of the average plaquette at several values of β.

Fig. 3.3. The evolution of the Z_2 gauge theory from an ordered start at $\beta = 0.425$.

Fig. 3.4. The evolution of the totally ordered and disordered states at $\beta = \beta_c$ for Z_2 gauge theory.

Fig. 3.5. The average plaquette as a function of β in a thermal cycle on a). SU(2) in five dimensions, b). SU(2) in four dimensions and c). $SO(2) \equiv U(1)$ in four dimensions. Crosses, heating; circles, cooling.

Fig. 3.6. Wilson loops for SU(2) at $\beta = 3$ as a function of lattice size.

Fig. 3.7. The quantities X(I,J) for SU(2) gauge theory as a function of $1/g_o^2$.

Fig. 3.8. The quantities X(I,J) for SU(3) gauge theory.

Fig. 4.1. Graphical interpretation of eqs. 4.11 and 4.12 for an asymptotically free theory.

Fig. 4.2. An example of a non-trivial fixed point.

Fig. 4.3. The quantities F and G for the SU(2) theory.

Fig. 4.4. The quantities F and G for the U(1) theory.

Fig. 4.5. Testing the prediction of asymptotic freedom.

Fig. 4.6. The inverse renormalized charge squared at r = 2a versus the inverse bare charge squared for the SU(2) theory.

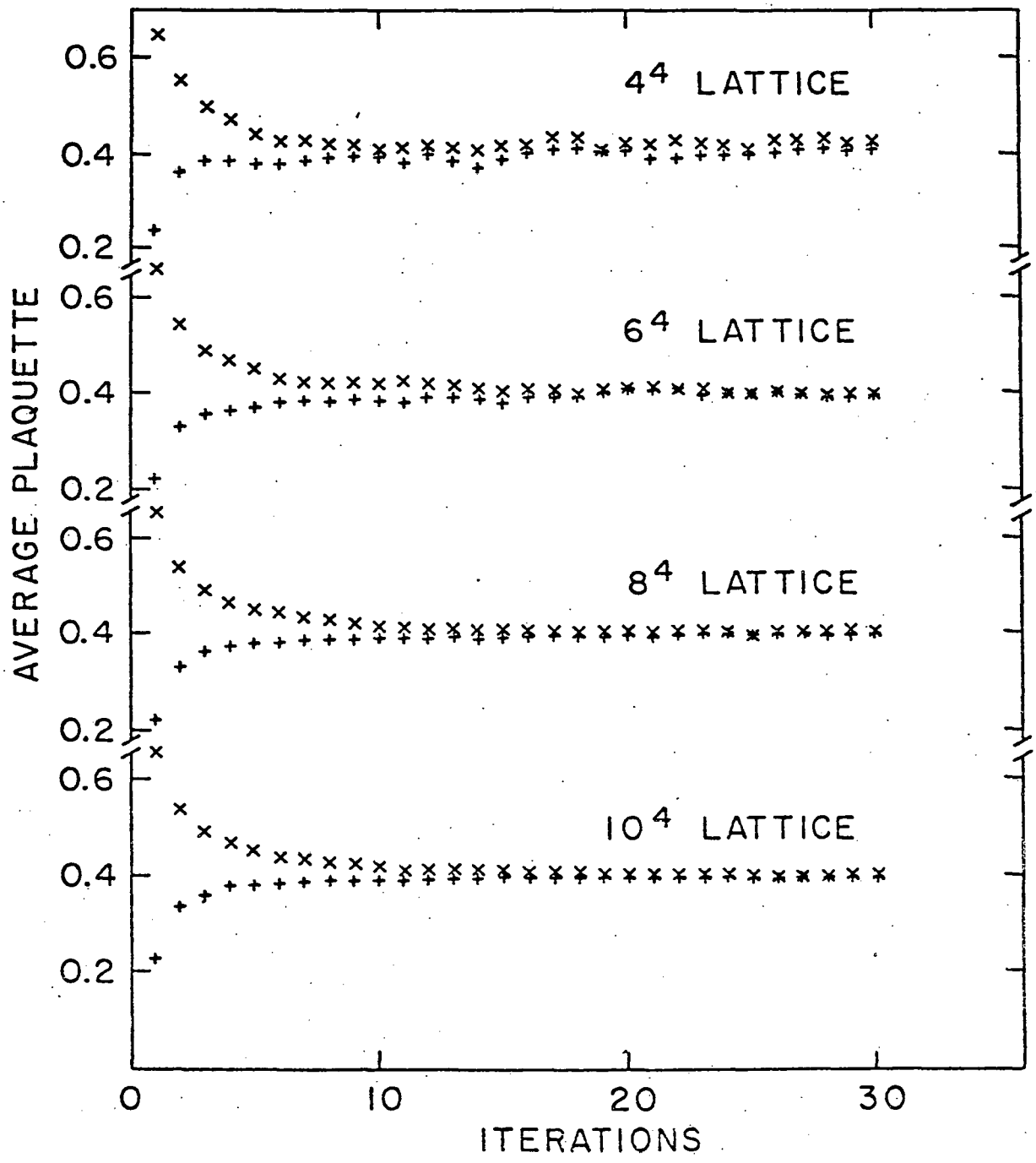
AVERAGE PLAQUETTE
0.6
0.4
0.2
4^4 LATTICE
6^4 LATTICE
8^4 LATTICE
10^4 LATTICE
0
10
20
30
ITERATIONS

Figure 3.1

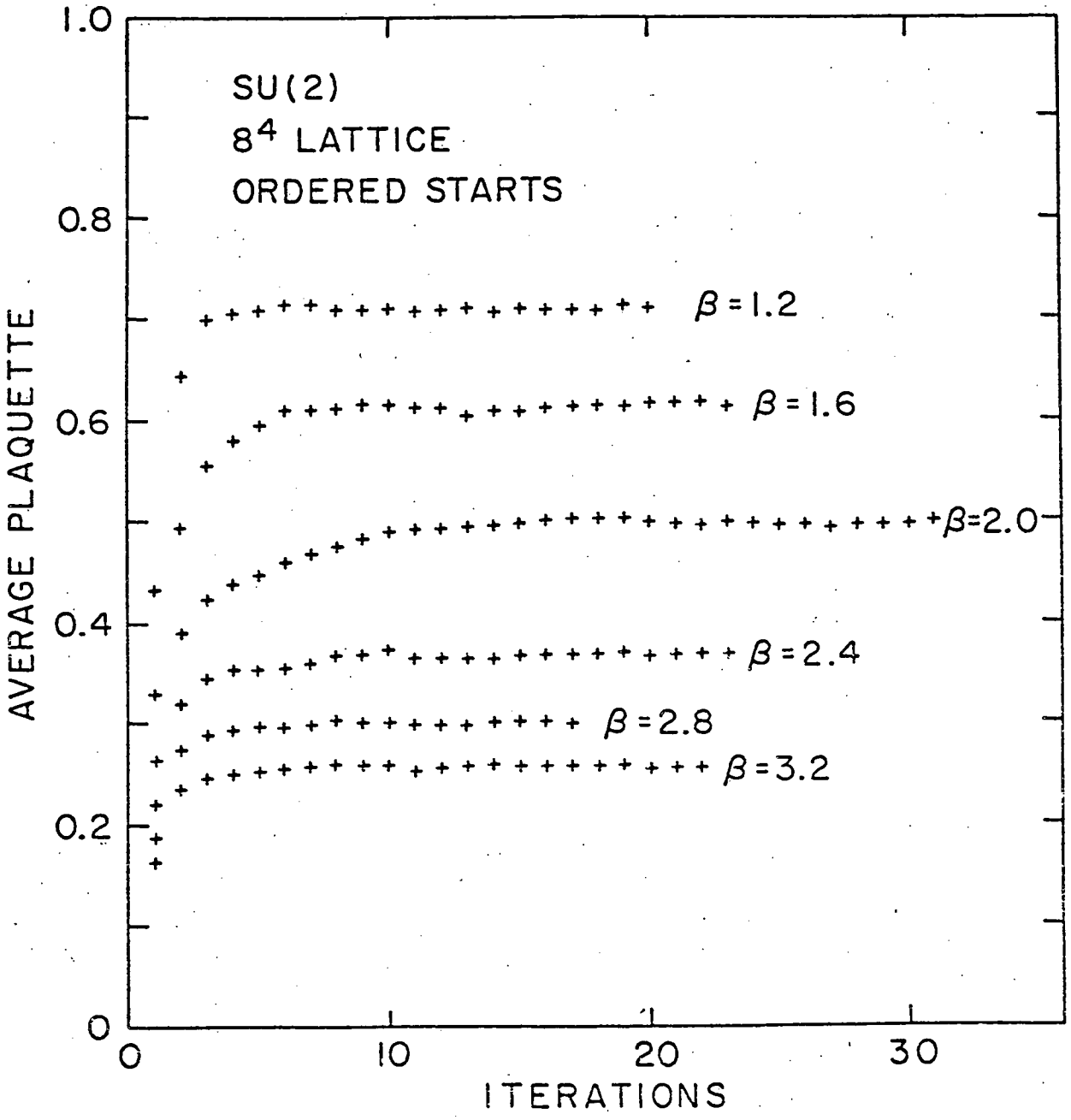
SU(2)
8^4 LATTICE
ORDERED STARTS
$\beta = 1.2$
$\beta = 1.6$
$\beta = 2.0$
$\beta = 2.4$
$\beta = 2.8$
$\beta = 3.2$
AVERAGE PLAQUETTE
ITERATIONS
1.0
0.8
0.6
0.4
0.2
0
0
10
20
30

Figure 3.2

THIS PAGE

WAS INTENTIONALLY

LEFT BLANK

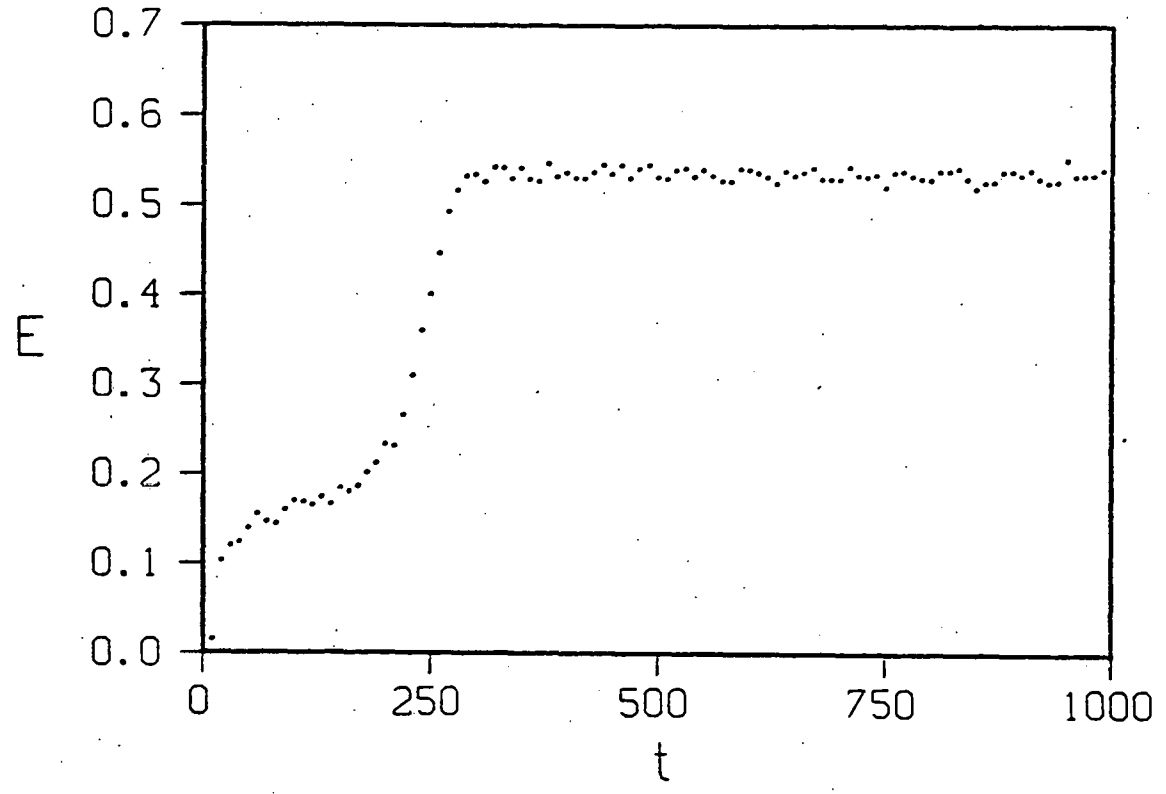

Figure 3.3

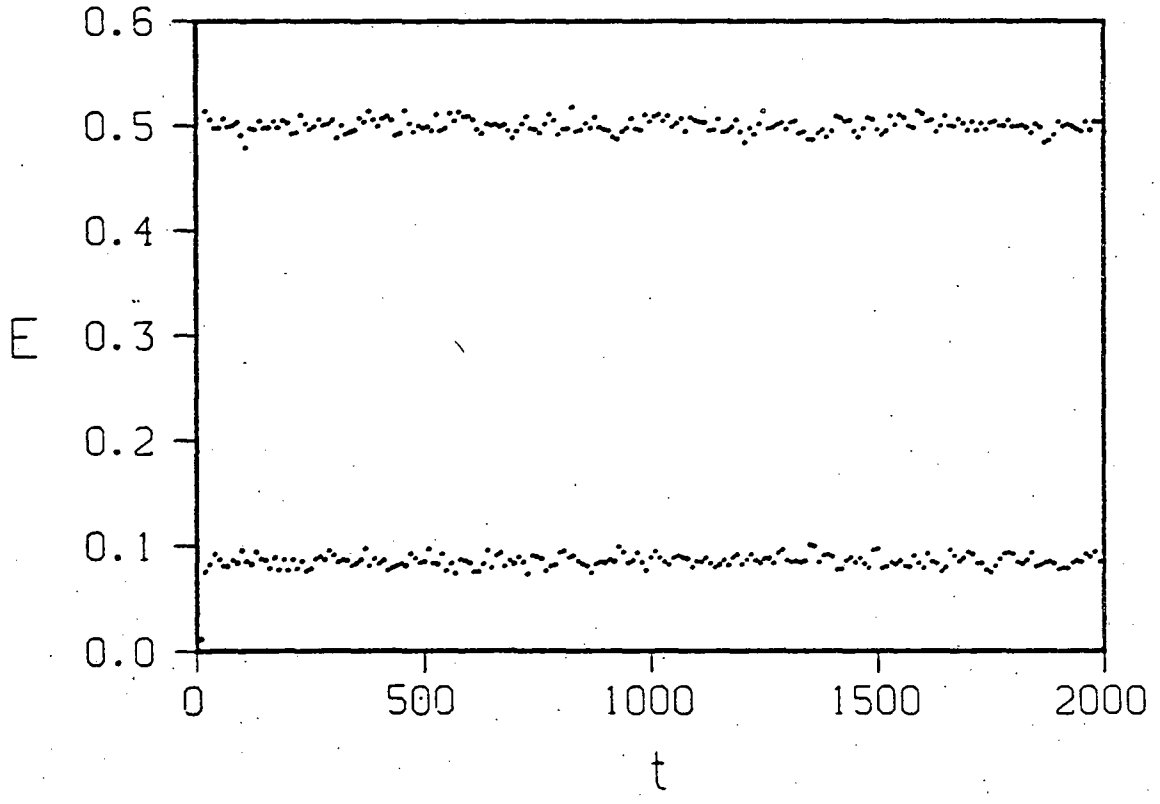

Figure 3.4

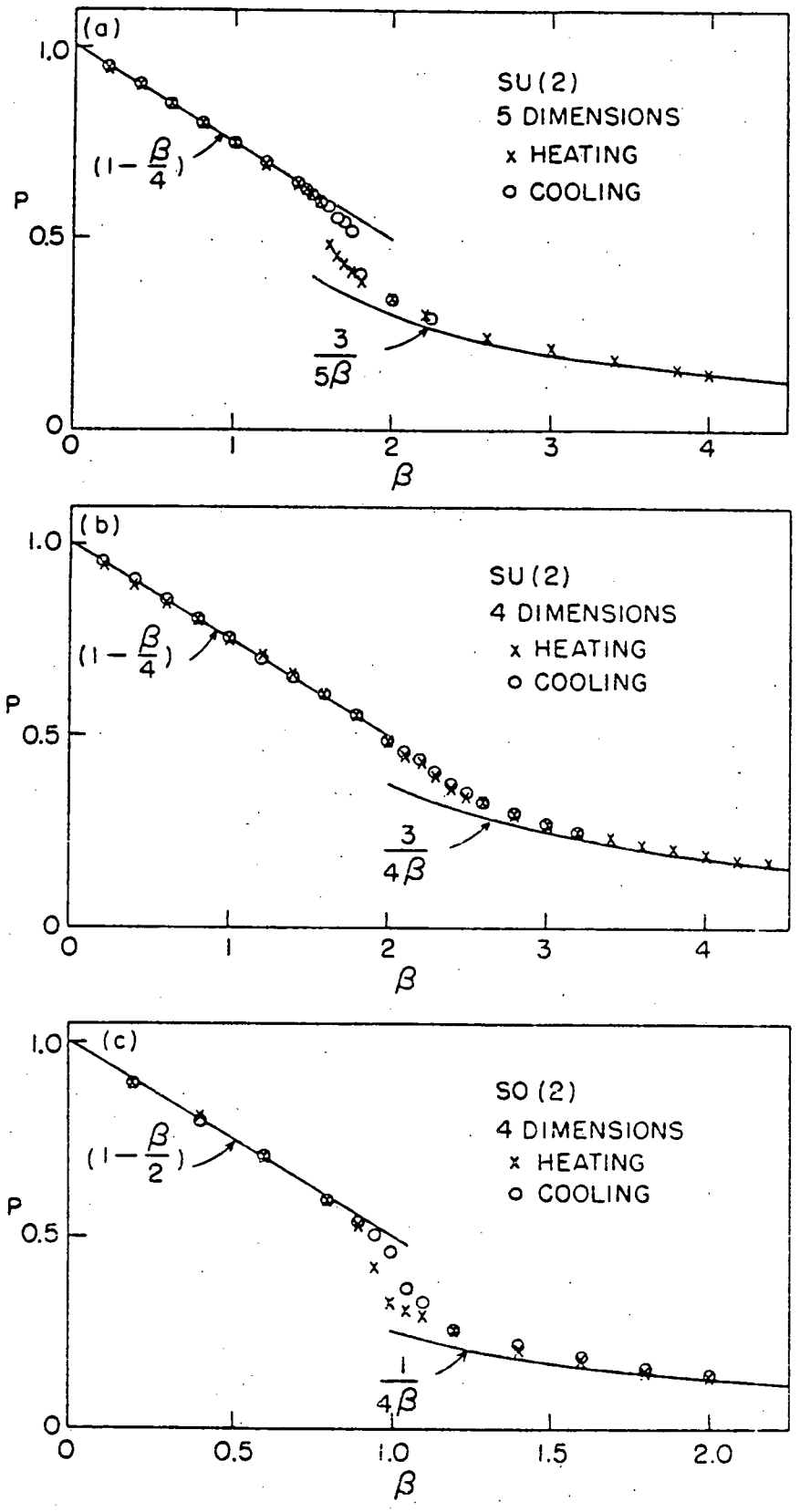
(a)
SU(2)
5 DIMENSIONS
x HEATING
o COOLING
$(1-\frac{\beta}{4})$
$\frac{3}{5\beta}$
P
β
(b)
SU(2)
4 DIMENSIONS
x HEATING
o COOLING
$(1-\frac{\beta}{4})$
$\frac{3}{4\beta}$
P
β
(c)
SO(2)
4 DIMENSIONS
x HEATING
o COOLING
$(1-\frac{\beta}{2})$
$\frac{1}{4\beta}$
P
β

Figure 3.5

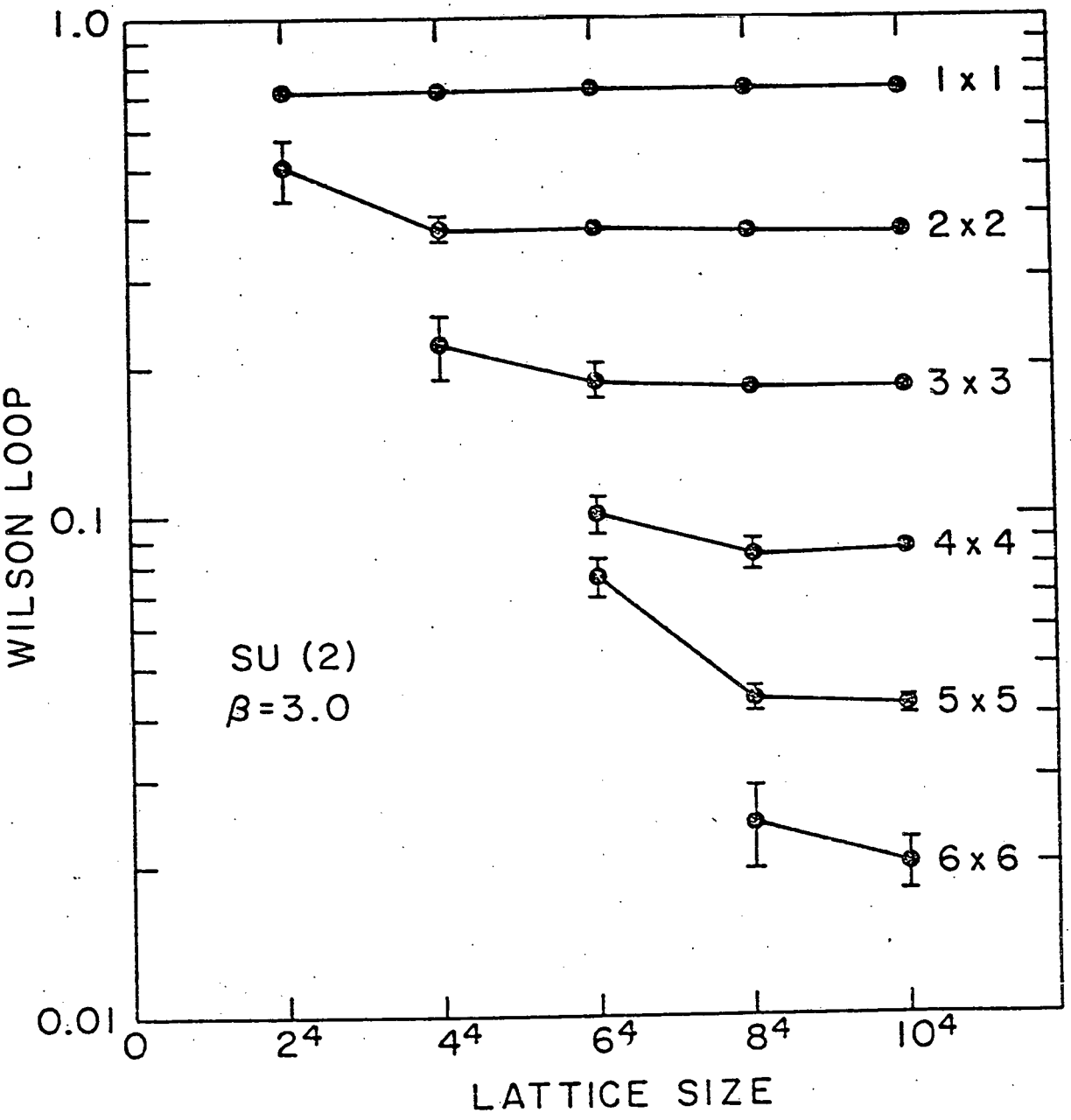
1.0
0.1
0.01
WILSON LOOP
SU (2)
β=3.0
1 x 1
2 x 2
3 x 3
4 x 4
5 x 5
6 x 6
0
2⁴
4⁴
6⁴
8⁴
10⁴
LATTICE SIZE

Figure 3.6

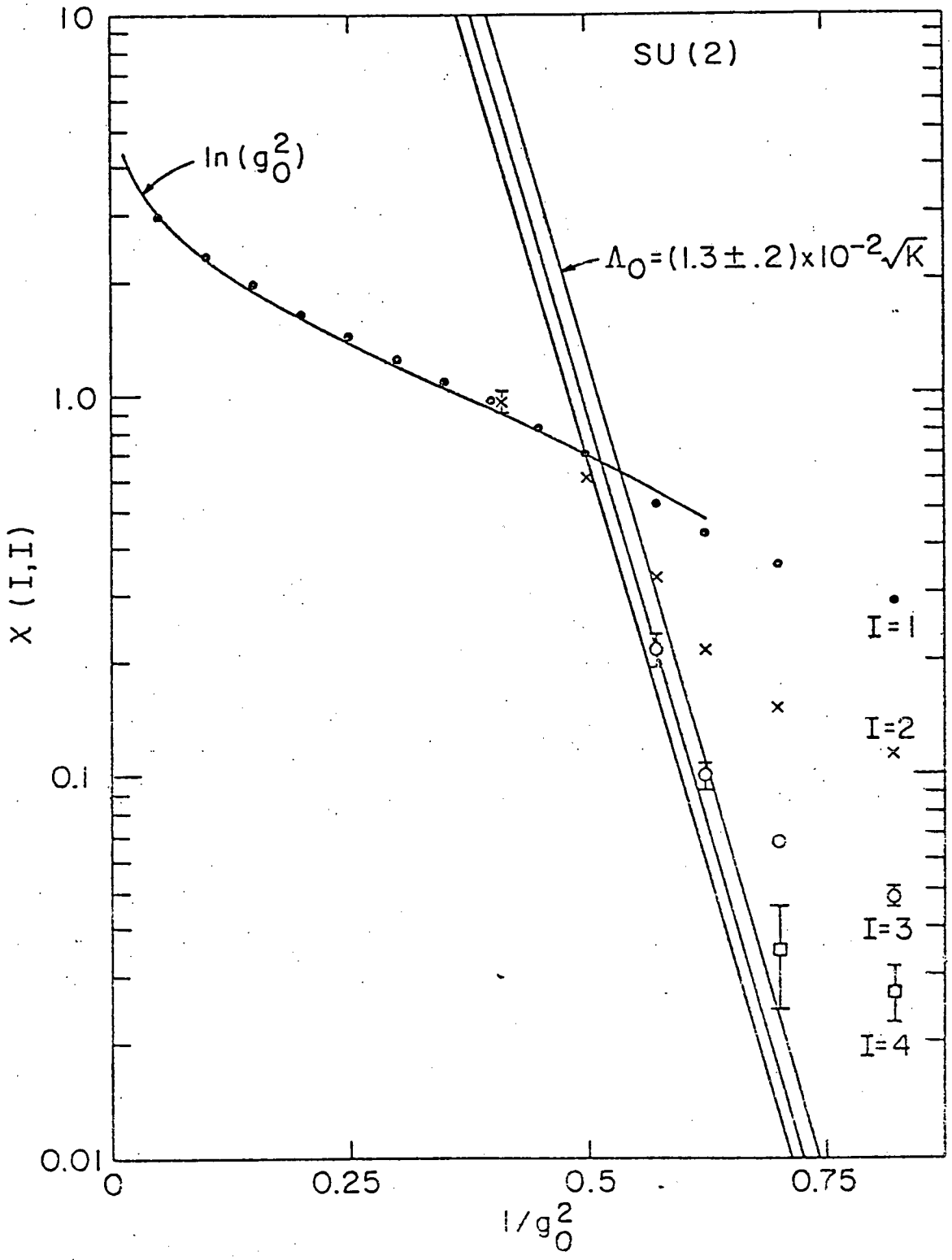
SU(2)
$\ln(g_0^2)$
$\Lambda_0=(1.3\pm.2)\times10^{-2}\sqrt{K}$
$\chi(I,I)$
$1/g_0^2$
10
1.0
0.1
0.01
0
0.25
0.5
0.75
I=1
I=2
I=3
I=4

Figure 3.7

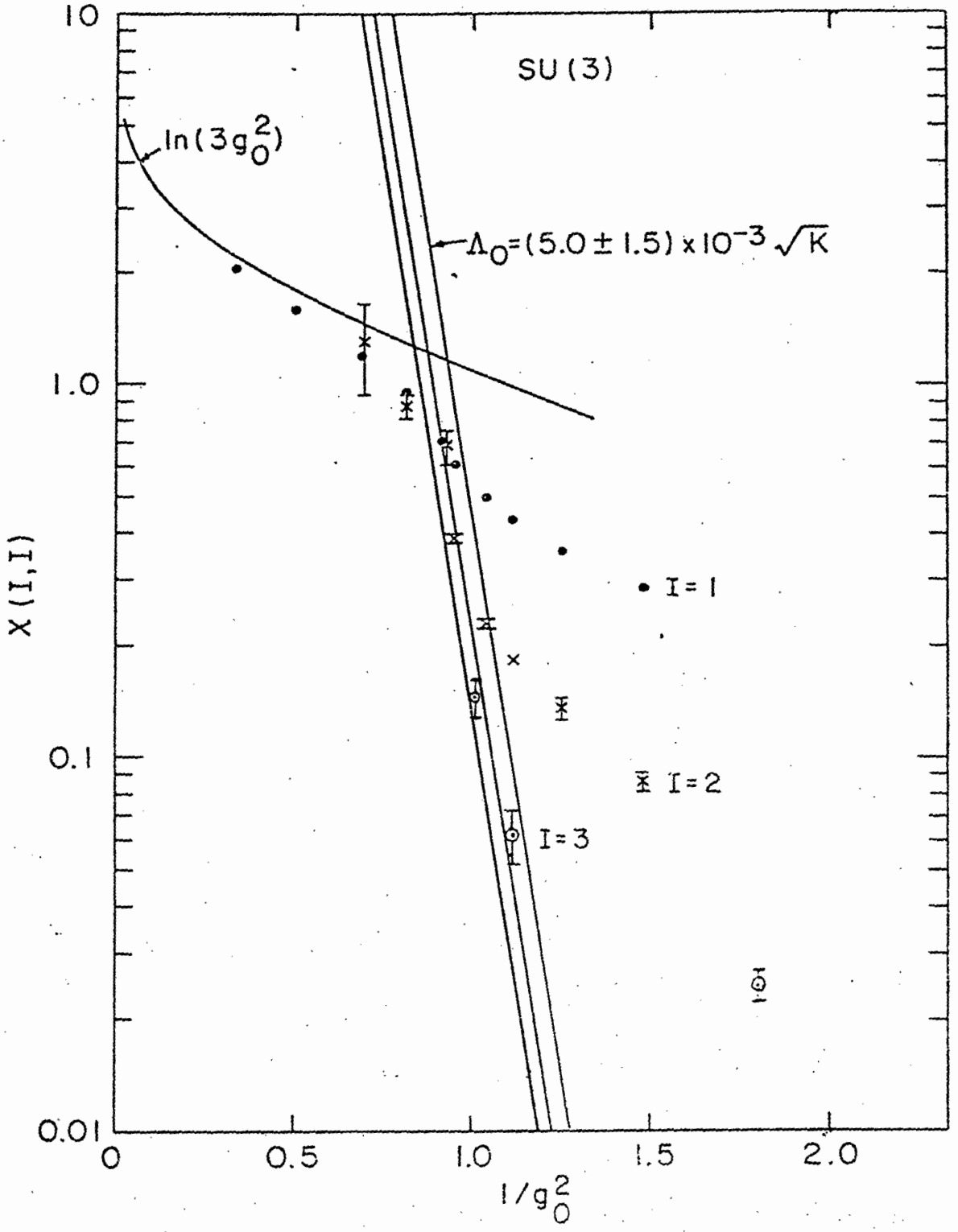
SU(3)
$\ln(3g_0^2)$
$\Lambda_0=(5.0\pm1.5)\times10^{-3}\sqrt{K}$
I=1
I=2
I=3
X(I,I)
$1/g_0^2$
10
1.0
0.1
0.01
0
0.5
1.0
1.5
2.0

Figure 3.8

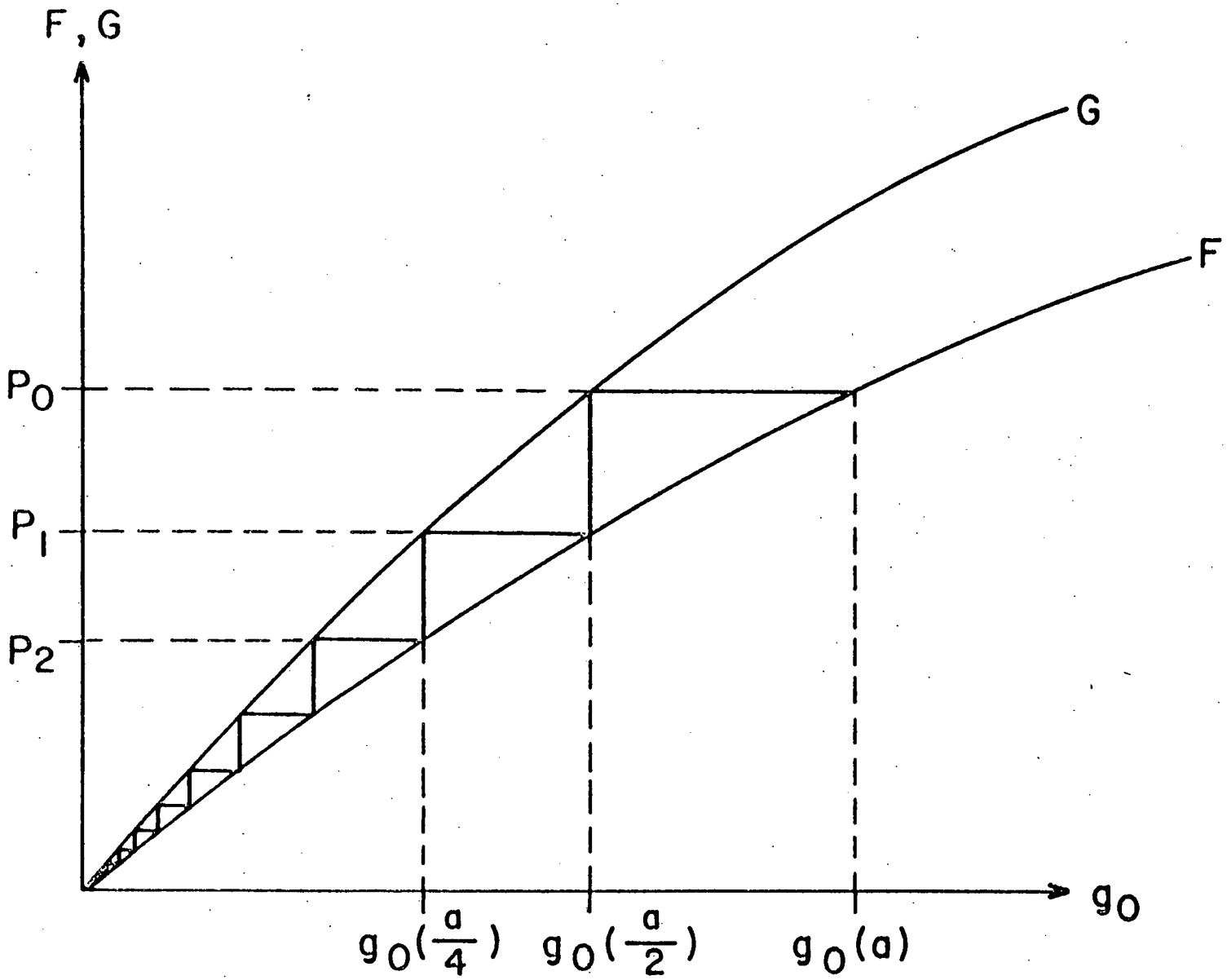

Figure 4.1

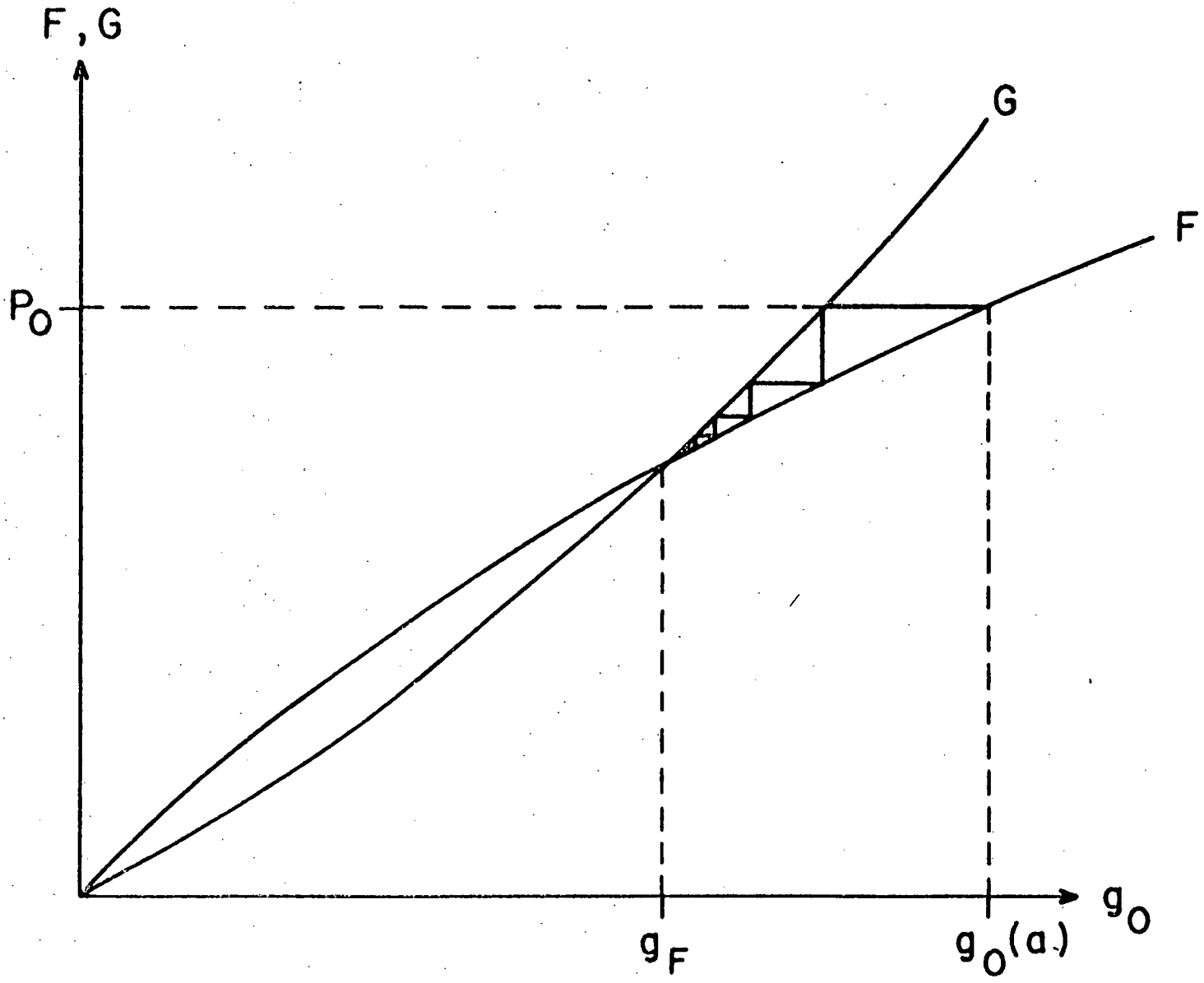

Figure 4.2

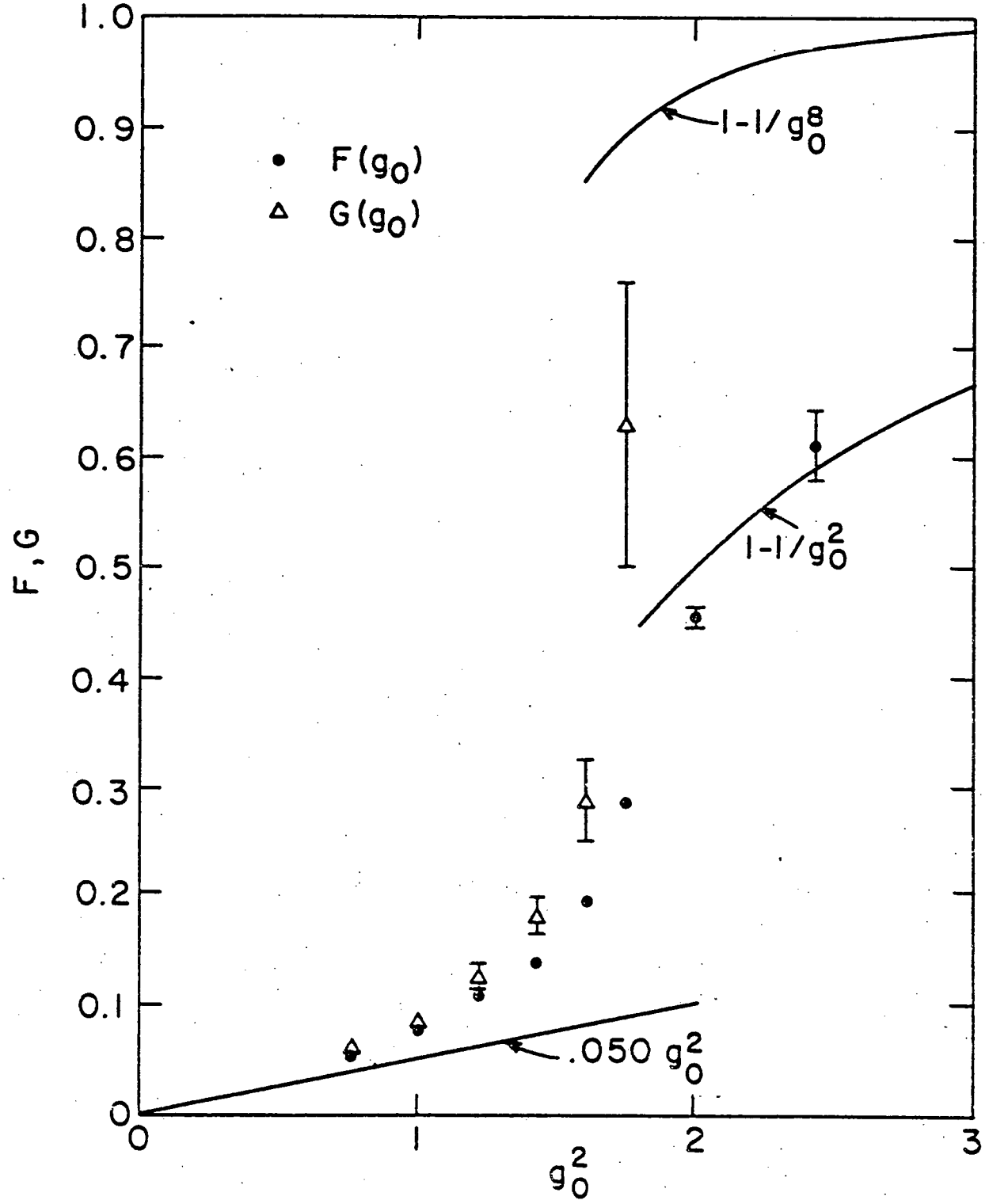
1.0
0.9
0.8
0.7
0.6
0.5
0.4
0.3
0.2
0.1
0
F, G
F(g0)
G(g0)
1-1/g0^8
1-1/g0^2
.050 g0^2
0
1
2
3
g0^2

Figure 4.3

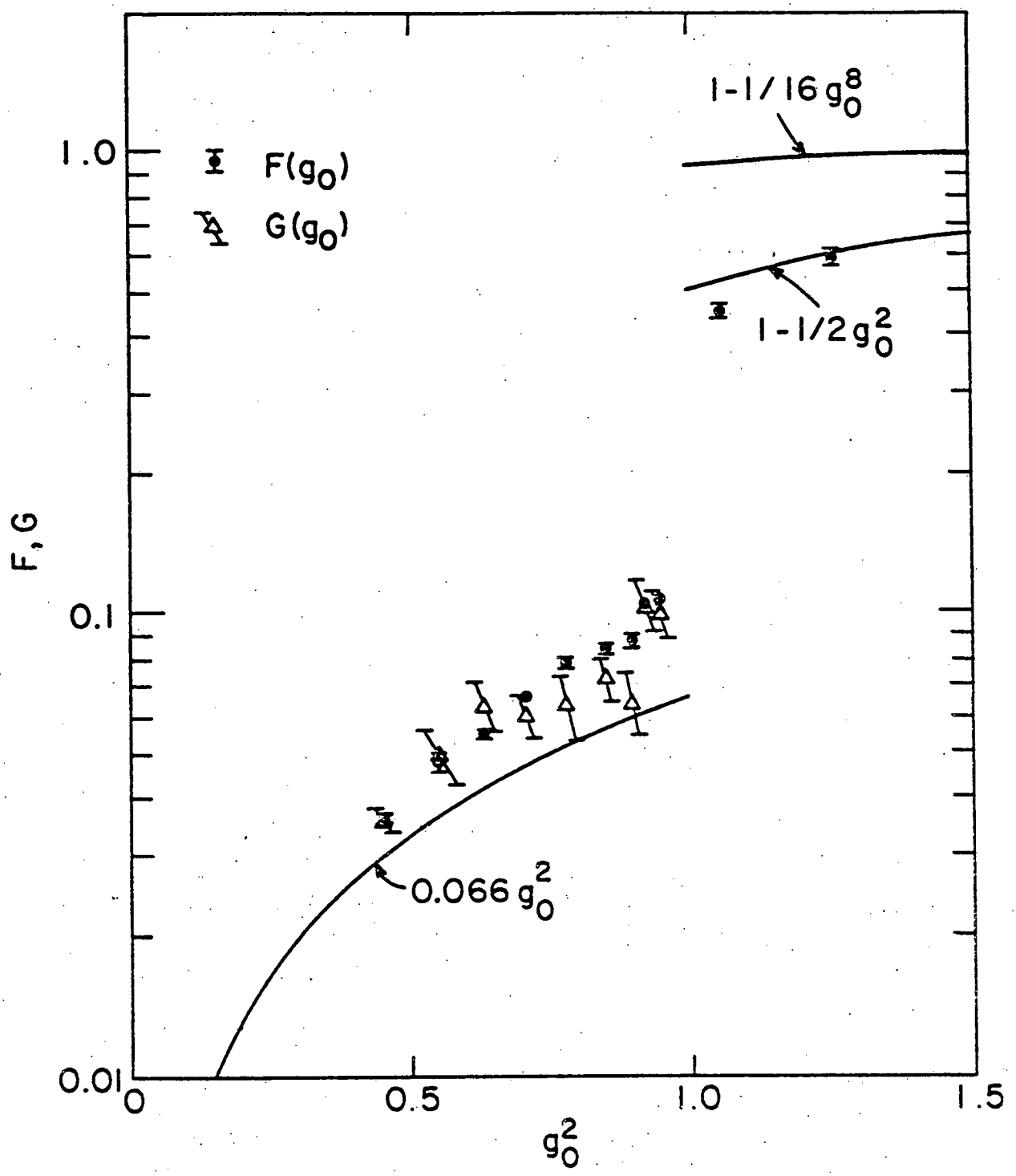

Figure 4.4

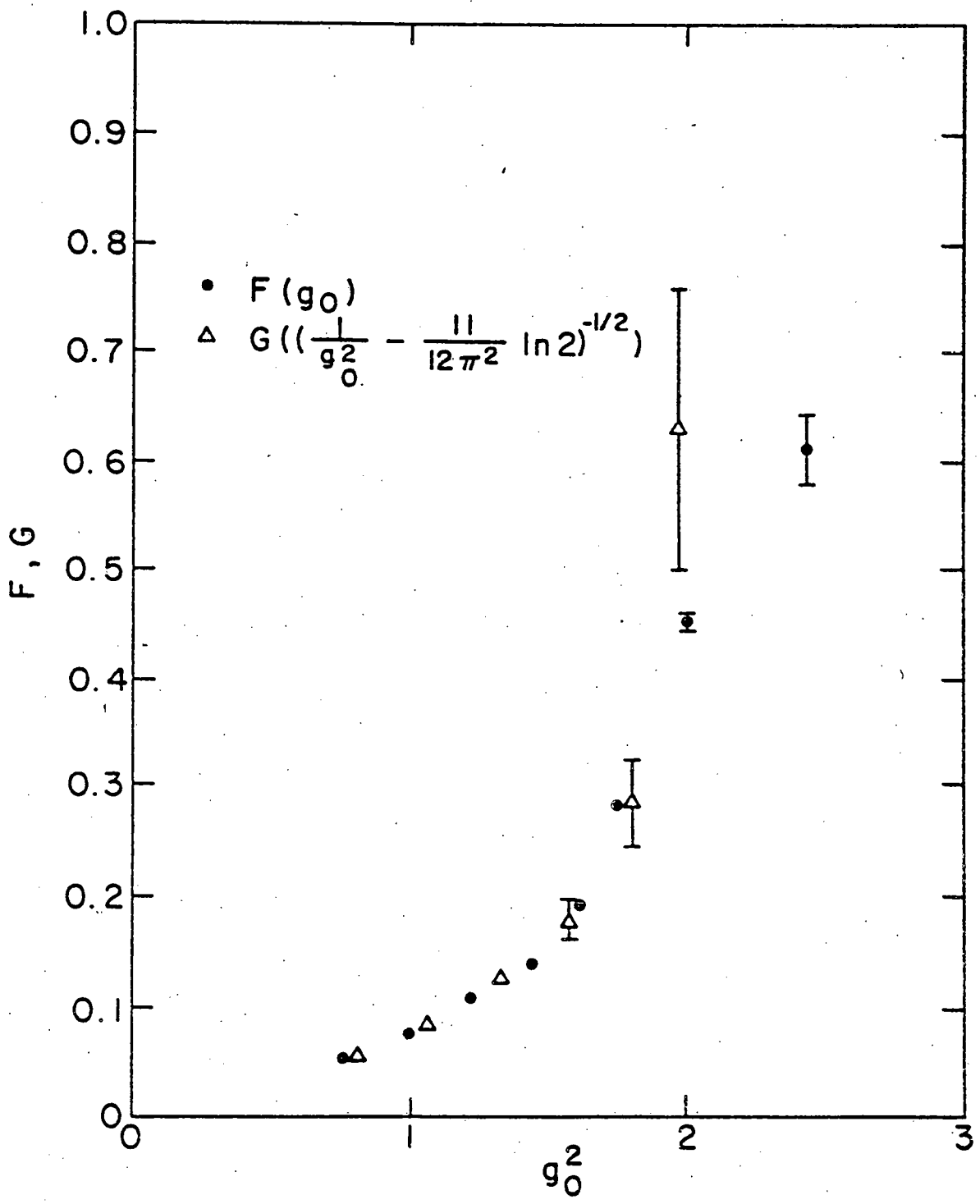

Figure 4.5

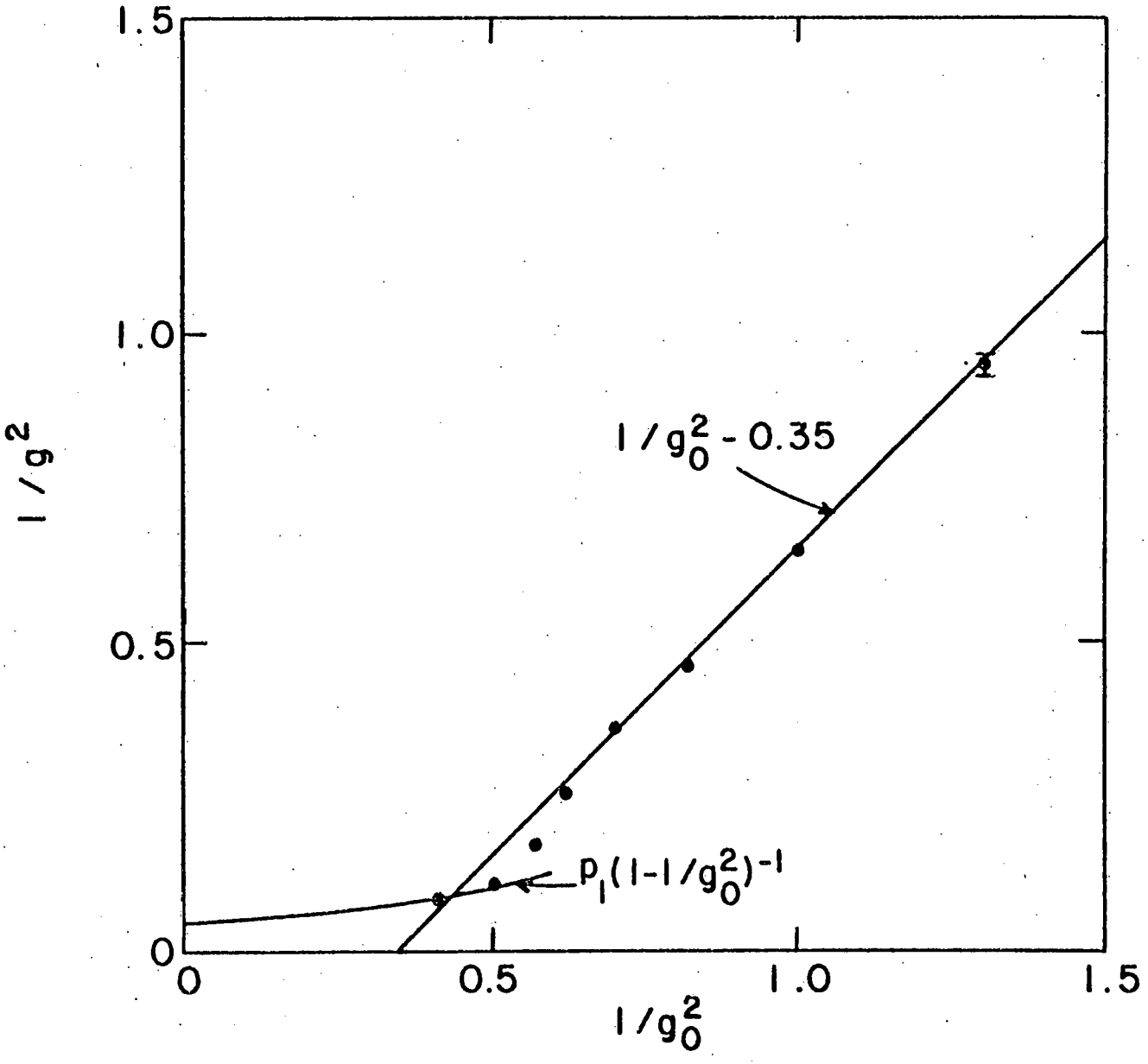

Figure 4.6